CHINESE OPTICS LETTERS

Vol. 22, No. 4 | April 2024

Optical pulse repetition rate division using an optoelectronic oscillator

Ping Li (李 平), Kunlin Shao (邵琨麟), Yamei Zhang (张亚梅)*, and Shilong Pan (潘时龙)

National Key Laboratory of Microwave Photonics, Nanjing University of Aeronautics and Astronautics, Nanjing 210016, China

*Corresponding author: zhang_ym@nuaa.edu.cn

Received November 16, 2023 | Accepted January 2, 2024 | Posted Online April 25, 2024

An approach for frequency division of an optical pulse train (OPT) based on an optoelectronic oscillator (OEO) is proposed and experimentally demonstrated. When the OPT is injected into the OEO, a microwave signal with a frequency equaling fractional multiples of the repetition rate of the OPT is generated. This signal is then fed back to the OEO, maintaining its oscillation, while simultaneously serving as the control signal of a Mach–Zehnder modulator (MZM) in the OEO. The MZM acts as an optical switch, permitting specific pulses to pass through while blocking others. As a result, the repetition rate of the OPT is manipulated. A proof-of-concept experiment is carried out. Frequency division factors of 2 and 3 are successfully achieved. The phase noises of the OPT before and after the frequency division are investigated. Compared to previously reported systems, no external microwave source and sophisticated synchronization structure are needed.

Keywords: frequency division; optoelectronic oscillator; mode-locked laser; microwave photonics.

DOI: 10.3788/COL202422.043902

1. Introduction

Passive mode-locked lasers (MLLs) are capable of producing ultrafast femtosecond and picosecond optical pulse trains (OPTs) with extremely low timing jitters[1–3], which are vital in applications such as the generation and transmission of orthogonal frequency-division multiplexing signals[4], long-range active ranging[5], and high-capacity data transmission[6]. Various applications may require MLLs with different or tunable repetition rates. However, the repetition rate of a passive MLL is inherently determined by the length of the laser cavity[7]. To deal with this issue, considerable efforts have been dedicated to finding solutions. Instead of directly generating an OPT with a tunable repetition rate, a more effective method is to adjust the repetition rate outside the laser cavity. Recent studies[8–12] have proposed a technique for manipulating the repetition rate of an OPT based on the temporal Talbot effect using a dispersive element. By carefully designing the dispersion of the dispersive element, the repetition rate of a 9.7-GHz OPT is successfully halved[10]. However, considering an OPT with a 100-MHz repetition rate, a dispersive element with a dispersion value exceeding 5×10^6 ps/nm is required to obtain a frequency division factor of 2, which would result in a severe power loss. In addition to this method, the frequency manipulation of the OPT can also be simply realized by using an optical switch[13], but that requires synchronization between the driven signal of the optical switch and the OPT. Although an approach using a microwave photonic phase detector to precisely divide the repetition rate of an OPT has recently been demonstrated[14], an external radio-frequency (RF) source and a synchronization structure are still essential, making the system bulky and costly.

In this Letter, an approach for achieving OPT frequency division is proposed and experimentally demonstrated based on an optoelectronic oscillator (OEO). A stable microwave signal that is naturally synchronized with the OPT can be successfully generated by the OEO. The signal is fed back to the RF input of a Mach–Zehnder modulator (MZM) in the OEO, which jointly functions as an optical switch. The optical switch then selects one pulse out of every two or three pulses, and the remaining one or two pulses coincide precisely with the zero-crossing points of the optical switch. Frequency division of the OPT by two or three can be successfully achieved. An experiment is carried out. The repetition rate of the OPT, originally at 100.4 MHz, is successfully divided into 50.2 and 33.46 MHz. The proposed system eliminates the need for additional RF sources and synchronization structures, significantly reducing the complexity, cost, size, and power consumption of the system.

2. Principle

The schematic diagram of the proposed OPT frequency divider is illustrated in Fig. 1, which consists of an MLL, an MZM, an optical coupler (OC), a tunable optical delay line (TODL), a photodetector (PD), two bandpass filters (BPFs), an electrical amplifier (EA), a 10-dB directional electrical coupler (EC),

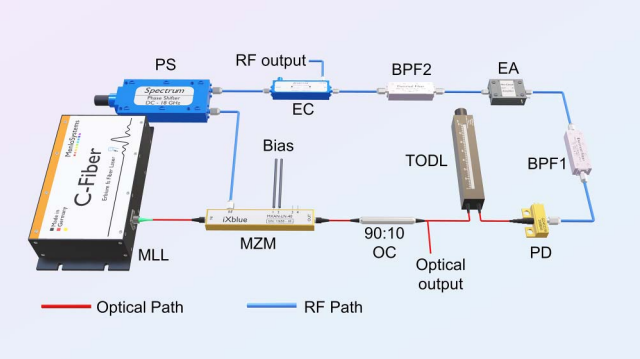

Fig. 1. Schematic diagram of the proposed OPT frequency divider. MLL, mode-locked laser; MZM, Mach–Zehnder modulator; OC, optical coupler; TODL, tunable optical delay line; PD, photodetector; BPF, bandpass filter; EA, electrical amplifier; EC, electrical coupler; PS, phase shifter.

and a phase shifter (PS). An OPT with a repetition rate of f_{rep} is produced by the MLL and is modulated by the oscillated signal from the OEO loop at the MZM. An OC divides the output of the MZM into two paths, and one path serves as the output of the frequency divider, while the other path stays in the loop for optoelectronic oscillation, which is incorporated into a PD to convert to the electrical domain after passing through a TODL. A BPF (BPF1) with an appropriate central frequency and a narrow bandwidth is followed to suppress the harmonics beaten from the MLL, and an EA is employed to compensate for the loop loss. Another BPF (BPF2) is then followed to remove excess noise induced by the EA. An EC splits the output of the EA into two paths, and one path is looped back to the RF port of the MZM via a PS to maintain the oscillation, and the other path works as the electrical output port of the total system. Connected to the RF output port is an electrical spectrum analyzer (ESA), allowing for the monitoring of the signal spectra and phase noise. When the oscillation stabilizes, a precise division of the OPT repetition rate can be achieved. The central frequency of the two BPFs plays an essential role in determining the final frequency of the microwave signal oscillated by the OEO.

To demonstrate the principle explicitly, mathematical derivation is conducted. Considering the complexity of the entire process of the OEO, only the steady state is considered here for the sake of simplicity. The OPT from the MLL can be expressed as an impulse function,

$$E_{\mathrm{pulse}}(t) = \sqrt{P}\sum_{n=0}^{\infty}\delta\left(t - n\frac{1}{f_{\mathrm{rep}}}\right), \tag{1}$$

where P is the peak power of each pulse, and n is an integer. The ideal central frequency of the BPF is $q \cdot f_{\mathrm{rep}}$, and q would determine the frequency division factor, equaling 1/2, 1/3, and 2/3. Therefore, the microwave signal derived from the OEO is expressed as

$$m(t) = A\ \sin(2\pi(N+q)f_{\mathrm{rep}}t + \varphi), \tag{2}$$

where A and φ represent the amplitude and phase of the microwave, respectively, and N is an integer. The transfer function of the MZM can be expressed as

$$h(t) = \cos\left(\frac{\pi a}{V_\pi}\ \cos(2\pi(N+q)f_{\mathrm{rep}}t) + \theta\right), \tag{3}$$

where a is the amplitude of the microwave, V_π and θ are the half-wave voltage and the bias phase of the MZM, respectively. As a result, the output of the MZM is obtained, as given by the following equation:

$$\begin{aligned} E(t) &= E_{\mathrm{pulse}}(t)\cdot h(t) \\ &= \sqrt{P}\sum_{n=0}^{\infty}\cos\left(\frac{\pi a}{V_\pi}\ \cos(2\pi nq) + \theta\right)\delta\left(t - n\frac{1}{f_{\mathrm{rep}}}\right). \end{aligned} \tag{4}$$

It can be found from Eq. (4) that when a and θ are chosen with appropriate values, the OPT can be frequency-divided. The two desired variables a and θ can be obtained from q. Taking q equaling 2/3 as an example, the OPT repetition rate can be divided by 3, and we can establish the following equations:

$$\begin{cases} \cos\left(\frac{\pi a}{V_\pi} + \theta\right) = 1 \\ \cos\left(\frac{\pi a}{V_\pi}\cos\left(2\pi\cdot\frac{2}{3}\right) + \theta\right) = 0 \\ \cos\left(\frac{\pi a}{V_\pi}\cos\left(2\pi\cdot 2\cdot\frac{2}{3}\right) + \theta\right) = 0 \end{cases}. \tag{5}$$

Equation (5) is solved, and a and θ are achieved,

$$a = -\frac{V_\pi}{3}, \qquad \theta = \frac{\pi}{3}. \tag{6}$$

Substituting the results into Eq. (4), we can obtain

$$E(t) = \sqrt{P}\sum_{n=0}^{\infty}\delta\left(t - 3n\frac{1}{f_{\mathrm{rep}}}\right). \tag{7}$$

It is evident from Eq. (7) that the repetition rate of the OPT is divided by 3. The deduction is similar when q equals 1/2 and 1/3. When q equals 1/3, the results for a and θ, as well as the frequency-divided result of the OPT, are the same as when q equals 2/3. When q equals 1/2, the corresponding results are

$$\begin{cases} a = -\frac{V_\pi}{4}, \theta = \frac{\pi}{4} \\ E(t) = \sqrt{P}\sum_{n=0}^{\infty}\delta\left(t - 2n\frac{1}{f_{\mathrm{rep}}}\right) \end{cases}. \tag{8}$$

From Eq. (8), it is found that the repetition rate of the optical pulse can be divided by 2 when a and θ are set at appropriate values.

A simulation is performed to verify the feasibility of the proposed frequency-division scheme. The initial repetition rate setting for the OPT is 150 MHz, and microwaves with frequencies of 75, 50, and 100 MHz, equivalent to $(N+1/2)\cdot f_{\mathrm{rep}}$, $(N+1/3)\cdot f_{\mathrm{rep}}$, and $(N+2/3)\cdot f_{\mathrm{rep}}$, are injected into the

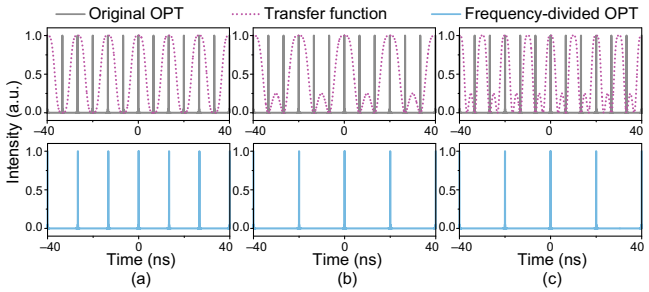

Fig. 2. Transfer function of the MZM, and the OPT before and after the frequency division with (a) 75-MHz driving signal, (b) 50-MHz driving signal, and (c) 100-MHz driving signal.

MZM, respectively. The simulation results are given in Fig. 2. The solid curves in gray and blue represent the OPT before and after the frequency division, respectively, while the purple dotted lines illustrate the transfer function of the MZM. In Fig. 2(a), a microwave signal with a frequency of 75 MHz is applied to the MZM, resulting in a halving of the original repetition rate of the OPT. Similarly, in Figs. 2(b) and 2(c), with microwaves of 50 and 100 MHz applied to the MZM, the repetition rate of the OPT is successfully divided by 3. It is worth noting that if the OPT and the microwave signal generated by the OEO are asynchronous, the pulses and the zero-crossing point of the optical switch cannot precisely coincide, leading to failed frequency division.

3. Experimental Results

An experiment based on the setup presented in Fig. 1 is carried out to verify the proposed system. An MLL (Menlo, C-Fiber) generates an OPT with a repetition rate of 100.4 MHz, which is sent to an MZM (iXblue, MXAN-LN-40) followed by an OC with a ratio of 90:10. The optical signal from the 10% port is injected into a PD after passing through a TODL, and the optical signal from the 90% port is coupled into an oscilloscope (OSC, Tektronicx, DSA72004B) with a sampling rate of 50 GSa/s to observe the time period and amplitude of the OPT. A BPF (BPF1) with a 3-dB bandwidth of 15 MHz is placed behind the PD. According to different q values, BPFs with different central frequencies are chosen. When q equals 1/2, 1/3, and 2/3, the central frequencies are 8.082, 8.065, and 8.098 GHz, respectively. An EA with a gain of 53 dB and another BPF (BPF2) with the same characteristics as BPF1 follow the BPF1. Before passing through the PS and being fed back to the MZM to construct the oscillation loop, a 10-dB directional EC is inserted to tap 10% of the RF signal power for observation purposes, which is linked to an ESA (Rode & Schwarz, FSWP50) to observe the frequency and stability of the interharmonics generated by OEO oscillation. As an example, when q equals 1/2, the repetition rate of the OPT is halved. To achieve this, adjustments are made to the PS (0°–360°), the bias voltage of the MZM, and the length of the TODL (0–660 ps) within the OEO loop. Successful division of the repetition rate by 2 times was confirmed when the interharmonic with a frequency of 8.082 GHz was displayed stably on the ESA interface, and the time period of the OPT exhibited on the OSC screen doubled from its original value. Similarly, for q equaling 1/3 and 2/3, the frequencies of the interharmonics are 8.065 and 8.098 GHz, respectively, corresponding to a repetition rate division factor of 3.

The solid lines in Fig. 3 illustrate the interharmonics spectra, ordered from top to bottom according to q values of 1/2, 1/3, and 2/3. The corresponding frequencies are 8.082, 8.065, and 8.098 GHz, respectively. The dashed lines in Fig. 3 represent the response curves of the BPFs. However, due to the limited suppression ratio of the BPFs at certain frequency points, there is the presence of spurious signals observed in Figs. 3(b) and 3(c). In Fig. 3(b), spurious signal frequencies are 8.032 and 8.098 GHz, aligning with the 80th harmonic and $(80\frac{2}{3})$th interharmonic of OPT. Figure 3(c) displays spurious signal frequencies of 8.065 and 8.132 GHz, corresponding to the $(80\frac{1}{3})$th interharmonic and 81st harmonic of OPT, respectively. The pulse envelopes and spectra of the OPT before and after the frequency division are recorded by the OSC and the ESA, shown in Fig. 4. In these subfigures, the black and colored lines represent the OPT before and after frequency division, respectively. It can be seen from Fig. 4 that the periods of the OPTs have been doubled and tripled, and the repetition rates of the OPTs have been reduced to half and one-third of the original value.

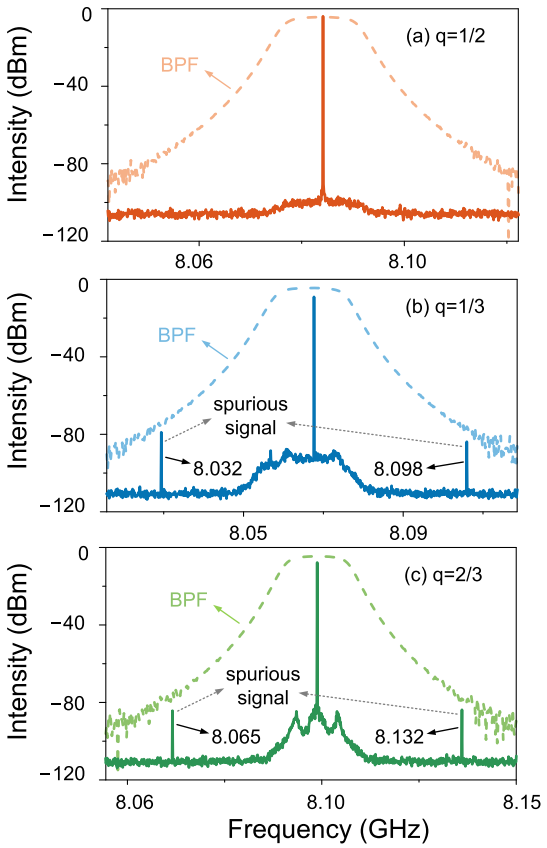

Fig. 3. Spectra of the interharmonics generated by OEO. (a) 8.082 GHz, (b) 8.065 GHz, (c) 8.098 GHz.

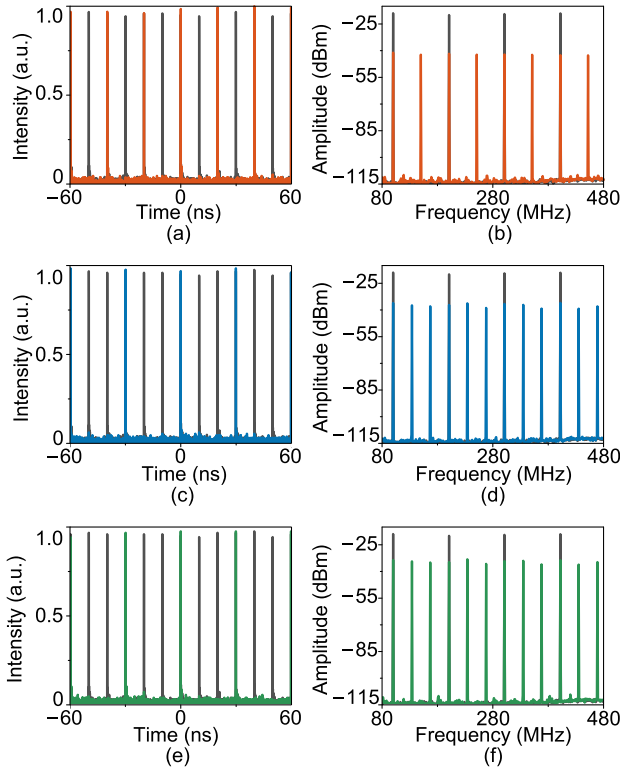

Fig. 4. (a) Waveform and (b) spectra of the OPT when q equals 1/2; (c) waveform and (d) spectra of the OPT when q equals 1/3; (e) waveform and (f) spectra of the OPT when q equals 2/3.

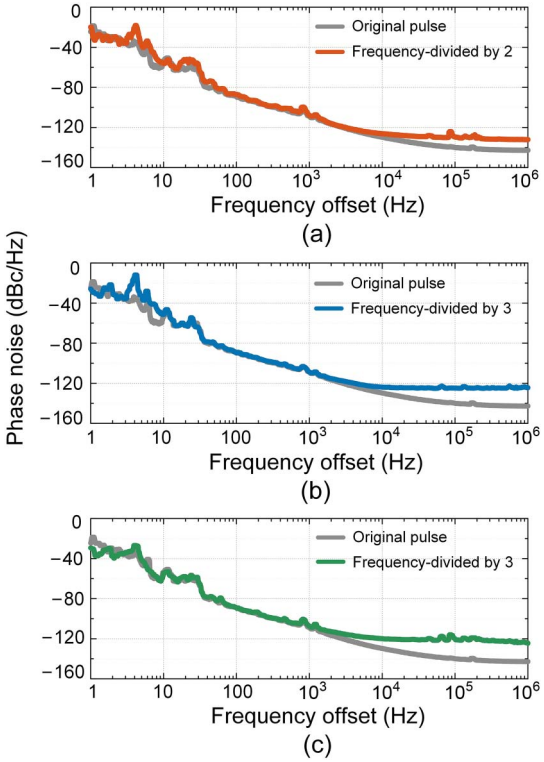

Fig. 5. Phase noise of the OPT before and after frequency division. (a) Frequency-divided by 2, (b) frequency-divided by 3, (c) frequency-divided by 3.

At the same time, the phase noise of the OPT before and after frequency division is investigated, with results displayed in Fig. 5. The gray lines represent the phase noise of the original OPT measured at 8.032 GHz, corresponding to the 80th harmonic. The colored lines represent the phase noise of the OPT after frequency division, measuring at 8.082, 8.065, and 8.098 GHz, respectively. Before sending the OPT after frequency division to the ESA, it undergoes filtering and amplifying. It is noteworthy that, prior to the 10-kHz frequency offset, the phase noise of the OPT before and after frequency division is basically consistent, indicating that the coherence of the OPT is good. However, at higher offset frequencies, the phase noise is higher than the original OPT, which is mainly attributed to the noise induced by the amplifier, which would be optimized in future experiments.

4. Conclusion

In conclusion, we have demonstrated an approach to achieving frequency division of OPT based on an OEO. Simulation and experimental results verified that the repetition rate of the OPT can be frequency-divided by 2 and 3 times without using additional RF sources and synchronization structures, thereby significantly reducing the system complexity. The phase noise of the OPT before and after frequency division remains consistent prior to a frequency offset of 10 kHz, showing that the system has a relatively good coherence. The proposed systems can be potentially employed in frequency-time distribution systems and synchronization systems.

Acknowledgements

This work was supported by the National Natural Science Foundation of China (Nos. 61901215 and 62271249) and the Fundamental Research Funds for the Central Universities.

References

1. A. Komarov, K. Komarov, and L. Zhao, "Broadband ultrashort pulses in passively mode-locked fiber lasers," Opt. Spectrosc. **128**, 493 (2020).
2. Y. Han, Y. Guo, B. Gao, *et al.*, "Generation, optimization, and application of ultrashort femtosecond pulse in mode-locked fiber lasers," Prog. Quantum. Electron. **71**, 100264 (2020).
3. Y. Mao, G. Liu, K. Zeb, *et al.*, "Ultralow noise and timing jitter semiconductor quantum-dot passively mode-locked laser for terabit/s optical networks," Photonics **9**, 695 (2022).
4. A. Delmade, T. Verolet, C. Browning, *et al.*, "Quantum dash passively mode locked laser for optical heterodyne millimeter-wave analog radio-over-fiber fronthaul systems," in *Optical Fiber Communications Conference and Exhibition (OFC)* (2020), p. 1.
5. R. Lamb, "A review of ultra-short pulse lasers for military remote sensing and rangefinding," Proc. SPIE **7483**, 748308 (2009).
6. G. Liu, Z. Lu, J. Liu, *et al.*, "Passively mode-locked quantum dash laser with an aggregate 5.376 Tbit/s PAM-4 transmission capacity," Opt. Express **28**, 4587 (2020).

7. H. Marco, J. Afonso, G. Sardiello, *et al.*, "Theoretical and experimental comprehensive study of GHz-range passively mode-locked fiber lasers," Appl. Opt. **59**, 6817 (2020).
8. J. Azaña and M. Muriel, "Temporal self-imaging effects: theory and application for multiplying pulse repetition rates," IEEE J. Sel. Top. Quantum Electron. **7**, 728 (2001).
9. J. Azaña and L. Chen, "General temporal self-imaging phenomena," J. Opt. Soc. Am. B **20**, 1447 (2003).
10. R. Maram, J. Howe, M. Li, *et al.*, "Noiseless intensity amplification of repetitive signals by coherent addition using the temporal Talbot effect," Nat. Commun. **5**, 5163 (2014).
11. L. Cortés, H. Chatellus, and J. Azaña, "On the generality of the Talbot condition for inducing self-imaging effects on periodic objects," Opt. Lett. **41**, 340 (2016).
12. B. Crockett, L. Cortés, R. Maram, *et al.*, "Optical signal denoising through temporal passive amplification," Optica **9**, 130 (2022).
13. O. Vries, T. Saule, M. Plötner, *et al.*, "Acousto-optic pulse picking scheme with carrier-frequency-to-pulse-repetition-rate synchronization," Opt. Express **23**, 19586 (2015).
14. K. Shao, P. Li, Y. Zhang, *et al.*, "Optical pulse interharmonic extraction and repetition rate division based on a microwave photonic phase detector," Opt. Lett. **48**, 2074 (2023).